18th Australasian Fluid Mechanics Conference
Launceston, Australia
3-7 December 2012

On the design of a recently constructed 285 m^3/s wind tunnel at the University of Adelaide

P. V. Lanspeary[1] **and R. M. Kelso**[1]

[1]School of Mechanical Engineering
University of Adelaide, South Australia 5005, Australia

Abstract

A closed-loop wind tunnel has been constructed on a floor area of 18.7×30.6 m^2 at the Thebarton campus of the University of Adelaide. The wind tunnel is for use by researchers and industrial clients of the university. There are two test sections in series. The larger of the two, with a 3.0×3.0 m^2 cross section and a length of 14.8 m is intended for wind engineering and sports science. The smaller of the test sections, which has a cross section of 2.75×2.0 m^2, is located at the outlet of a 4:1 contraction, and so is better suited to aerodynamics and aeroacoustics. The flow is driven by six fans, each with a diameter of 1.4 m. Design calculations predict a maximum flow rate of 285 m^3/s, giving 32 m/s in the wind-engineering section and 52 m/s in the aerodynamics test section.

Motivation and history

The years since 2000 have been a time of expansion for teaching and research in mechanical engineering at the University of Adelaide, with new courses in aeronautical, automotive, sports and sustainable-energy engineering. Early in this period it became apparent that South Australia lacked research and development facilities for industrial and aeronautical aerodynamics. However, after an internal feasibility study, funding for the construction of a large wind tunnel became available in early 2007.

From that point, the requirements were for a wind tunnel which would be useful to as many different disciplines of engineering as possible. The objective was to build a wind tunnel with size and flow speeds similar to those of the large wind tunnels at Monash University, RMIT University and DSTO in Melbourne.

Preliminary design

In early 2010, a building with a floor area of 18.7×30.6 m^2 became available. The building was somewhat smaller than initially invisaged, and so it became important to make best possible use of this space. To overcome the limitations of a 3.7 metre ceiling height, the larger parts of the wind tunnel would be constructed in large pits.

The preliminary design, which is a plan view of a closed-loop wind tunnel, is shown in Figure 1. In this design, there is a wind-engineering test section on the discharge side of the fans and an aerodynamics test section on the intake side of the fans. Flow through both test sections is conditioned by a honeycomb and wire-mesh screens, but the 4:1 contraction gives the aerodynamics section a much better uniformity and a much lower turbulence intensity in the core flow. The 3×2 m^2 aerodynamics section can be replaced with a smaller 2.1×1.4 m^2 test section, giving a higher flow speed, or it may simply be removed, leaving an open jet flow. The wind-engineering section is as long as practicable, and there are suitable roughness elements on the floor, so that the simulated atmospheric boundary layer is as thick as possible. It is also equipped with a turntable.

The preliminary design work determined that 6 direct-drive fans, each 1.4 m in diameter, would be less expensive than a single, larger fan of equivalent performance. These fans produce an unusually large pressure rise because the tip/hub diameter ratio is large (0.63) and the discharge flow is straightened by stator blades extending over the full length of the electric motors. At this stage it was also clear that, due to the high cost of connection to the public electricity grid, electrical power would be supplied by one or more diesel generators. Silencers are installed so that the wind tunnel becomes more useful for aeroacoustics research. There are turning vanes in each corner.

Design for Minimum Pressure Loss

Given the general arrangement in Figure 1, the main objective for the design detail is to minimise stagnation-pressure loss due to flow separation and secondary flow. Particular attention is therefore given to design of the duct components which have a propensity for generating large pressure loss — for example, corners and diffusers (or expansions). However there is not enough space to achieve minimum pressure loss with radiused corners and simple diffusers (Figure 2). All corners are therefore fitted with turning vanes. The effective cone angle (ϕ) of diffusers is kept sufficiently small either by designing them as part of the fan-discharge ducts, or by dividing the larger main duct into smaller side-by-side channels. Also, to minimise the need for diffusers, there is only one contraction.

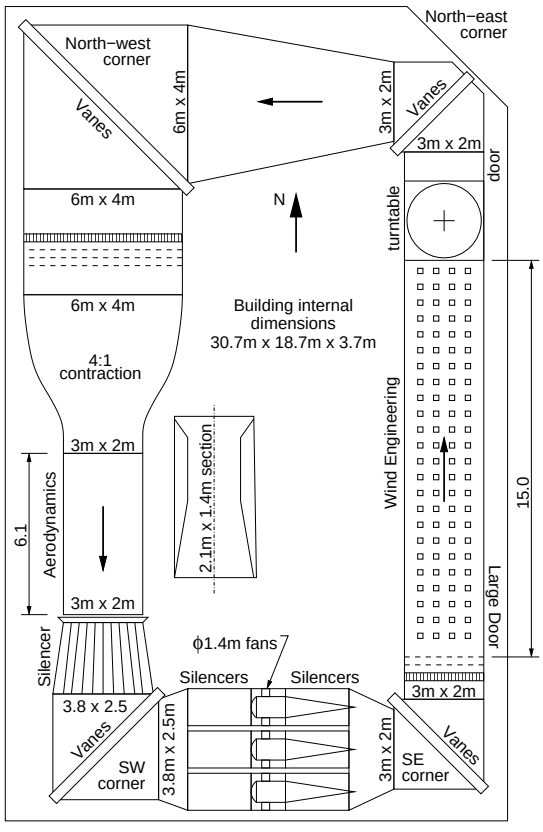

Figure 1: General arrangement (plan view) from the preliminary design.

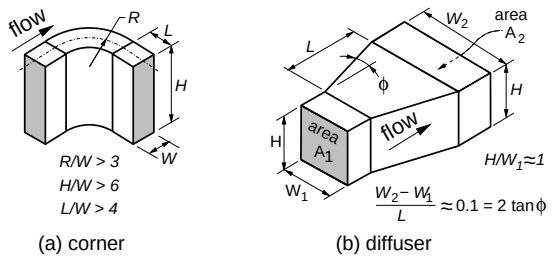

(a) corner (b) diffuser

Figure 2: Shape required for minimum pressure loss in radiused corners and simple diffusers [6, 7].

General Arrangement

The general arrangement of the wind tunnel in December 2012 is shown in Figures 3 and 4. Electrical power for the fans is provided by a 400 kW diesel generator. The electrical wiring makes provision for a second 400 kW generator (which is currently not installed). Calculations using pressure-loss coefficients and other data from the engineering literature give a maximum "as designed" flow rate (with 2 generators) of 285 m^3/s.

Corners

The south-west (SW) and south-east (SE) corners of the wind tunnel are designed as manifolds which join the fan-discharge ducts and fan-intake ducts to the test sections. As a consequence, the SW and SE corners are structurally complex but, also as a consequence, space is made available for efficient fan-

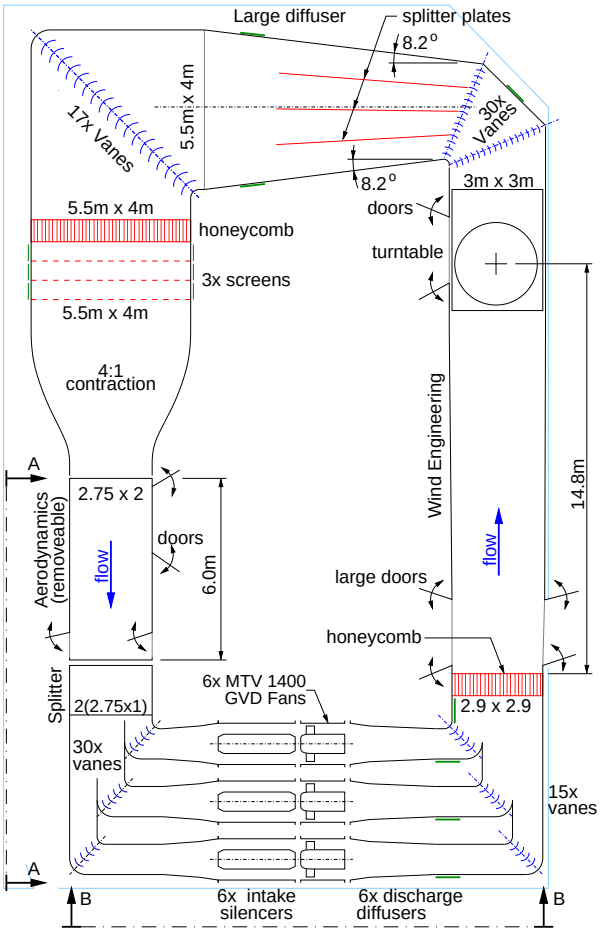

Figure 3: Simplified general arrangement of the wind tunnel (plan view). See Figure 4 for elevations AA and BB.

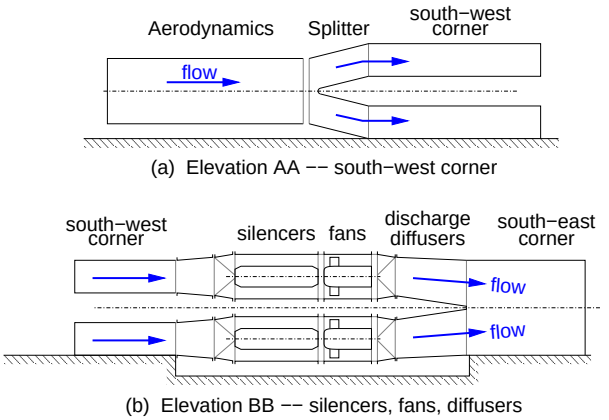

Figure 4: Simplified elevations of (a) south-west corner, (b) silencers, fans and discharge diffusers.

discharge diffusers. Also, as shown in Figure 4, the duct splits into an upper channel and a lower channel immediately downstream of the aerodynamics test section, thus making it possible to install standard commercial silencers at the fan intakes.

At the truncated north-east corner of the building, there are two rows of turning vanes. The first row of vanes turns the flow through an angle of 45°. Flow from the second row enters the diffuser without any intervening parallel-sided duct, and so the vanes in the second row are all different, with the angle of turn varying from 37.8° to 52.2°.

Turning vanes

With the use of turning vanes, minimum pressure losses are obtained in compact mitred corners. In small wind tunnels, the usual practice is for turning vanes to be a single thickness of curved sheet metal. These are simple to make and, with care, a loss coefficient of 0.1 can be achieved [8]. In a larger wind tunnel such as this, the turning vanes are thick aerofoils in order to obtain the required strength and rigidity. By using the vane geometry of Collar [3], which gives a constant-width channel between the vanes, we expect a loss coefficient of 0.05.

Figure 5(a) and the following constraints define the profile of the Collar turning vane:

$$\theta_2 = \theta_1, \quad (1)$$

$$R_i = 0.72S, \quad (2)$$

$$R_o = R_i + S\cos\theta_2 - 2.1t, \quad (3)$$

$$R_{le} \approx (S + R_i - R_o)/6, \quad (4)$$

where t is the thickness of the (sheet-metal) skin. The other symbols are defined in the diagram.

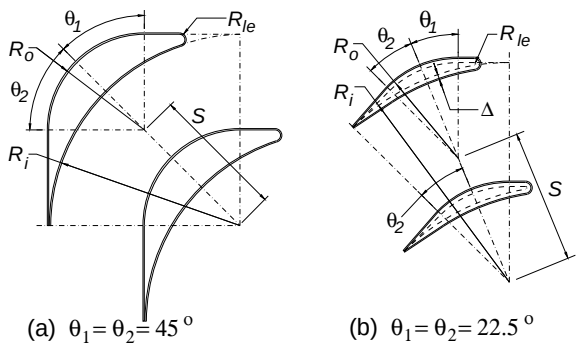

Figure 5: Constant-channel-width turning-vane profiles; (a) 90° turn (after Collar [3]); (b) 45° turn (vane is thickened by 2Δ).

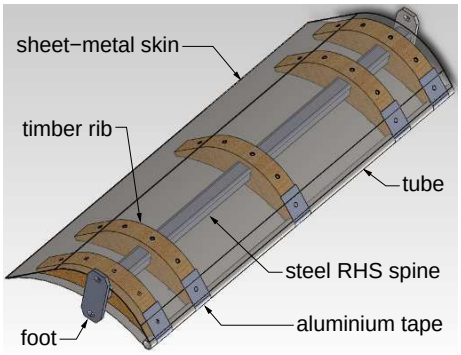

Figure 6: CAD image of SW-corner vane. To show internal detail the convex sheet-metal surface is rendered "transparent".

The turning angle of the flow can be changed simply by adjusting the values of θ_1 and θ_2. For example, $\theta_1 = \theta_2 = 22.5^\circ$ gives a 45° turning angle and, as shown by the dashed-line profile in Figure 5(b), the result is a much thinner vane. In the north-east-corner, where the vanes have a simply supported length of 3 m and the design flow speed is 33.3 m/s, the dashed-line profile would give insufficient flexural stiffness. Acceptable bending deflection is obtained by increasing the thickness of the vane. The increase in thickness is $2\Delta/S = 0.049$ over the front two thirds of the vane, and tapers to zero at the trailing edge.

Figure 6 illustrates the construction of a turning vane. Ribs of construction timber are pushed onto a RHS spine and a steel or aluminium tube provides the rounded leading edge. The sheet-metal skins are rolled to the required shape, screwed onto the ribs and then welded along their leading and trailing edges.

Test sections

The cross section of the wind-engineering test section expands slightly from 2.9×2.9 m^2 at the upstream end, to 3.0×3.0 m^2 at the turntable. The purpose of the expansion is to compensate for the displacement effect of boundary-layer growth along the length of the test section. At 285 m^3/s, the bulk flow speed at the turntable is 32 m/s.

The aerodynamics test section has a constant, non-adjustable 2.75×2.0 m^2 cross section and a length of 6.0 m. As recommended by the preliminary design, it is mounted on wheels so that, when removed, there is an open-jet flow from the contraction. At 285 m^3/s, the flow speed is 52 m/s.

Calibration and flow-characterisation measurements in both test sections are planned for early 2013.

Contraction

It is desirable, for the sake of a more uniform flow and lower turbulence intensity in the aerodynamics test section, to have a contraction with the largest possible area ratio. However, due to other requirements (e.g. for a large test section) and constraints (e.g. the size of the laboratory and cost) the practical limit for the area ratio is 4:1. To avoid boundary-layer separation, the length of the contraction is made equal to its inlet width ($L/W_1 = 1.0$)— as recommended by Chmielewski [2].

Bell and Mehta [1] have used the fifth-order polynomial

$$P(\xi) = 6\xi^5 - 15\xi^4 + 10\xi^3, \tag{5}$$

to define the shape of a wind-tunnel contraction. The roof, floor and side-wall profiles are then given by

$$\frac{H_1 - 2y}{H_1 - H_2} = \frac{W_1 - 2z}{W_1 - W_2} = P(\frac{x}{L}), \tag{6}$$

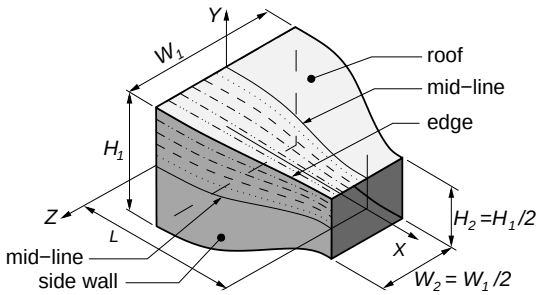

Figure 7: Contraction geometry: definition of coordinate system and dimensions; $H_1 = 4.00$ m, $W_1 = 5.50$ m, $L = 5.66$ m

where the (x,y,z) coordinate system and the other symbols are defined in Figure 7. The polynomial $P(\xi)$ is favoured for use as a contraction profile because its first and second derivatives vanish at the inlet and outlet planes. In the present case we modify the profile by applying a nonlinear transformation to streamwsise distance, x:

$$\frac{H_1 - 2y}{H_1 - H_2} = \frac{W_1 - 2z}{W_1 - W_2} = P\left(\left[\frac{x + x_o}{L + x_o}\right]^{1/n}\right), \tag{7}$$

with $n = 0.7$ and $x_o/L = 0.1$. Figure 8 shows that the transformation increases convex curvature near the outlet and moves the concave region away from the inlet.

In Figure 9, wall-pressure coefficients,

$$C_P = \frac{P - P_o}{\frac{1}{2}\rho U_o^2}, \tag{8}$$

which are obtained from potential-flow simulations, show regions of adverse pressure gradient near the inlet and outlet of the contraction. The reference conditions P_o, U_o are located in the duct far upstream of the contraction. Stratford [9] provides a convenient method of testing for turbulent-boundary-layer separation. With this method, separation occurs if

$$S(x) = C_p\sqrt{x\frac{dC_p}{dx}}\left(\frac{Re_x}{10^6}\right)^{-0.1} > \beta, \tag{9}$$

where $\beta = 0.39$. At a test-section flow speed of 5 m/s, the maximum value $S_{max} = 0.106$ is found at the edge of the contraction near the inlet, and is much smaller than required for separation.

Over the outlet plane of the contraction, the standard deviation of the simulation flow speed is 1.5% from the mean. This nonuniformity decays by a factor of 4 in 0.1 contraction lengths.

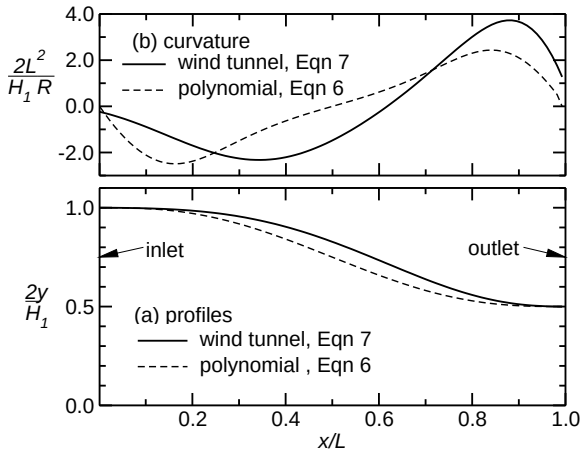

Figure 8: Profile and curvature of the wind tunnel contraction (Equation 7) and of the polynomial contraction, (Equation 6) [1]. R is radius of curvature.

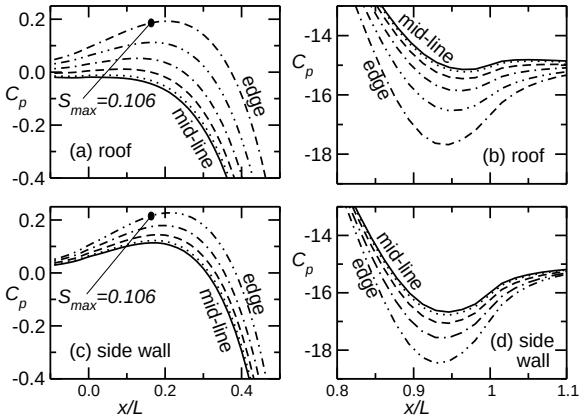

Figure 9: Pressure coefficients near regions of adverse pressure gradient, (a–b) on the roof and, (c–d) on the side-wall of the contraction. The location of maximum Stratford separation parameter, S_{max}, is shown with a •.

Honeycombs

Flow through the aerodynamics test section is conditioned by a honeycomb, a sequence of 3 wire-mesh screens and a 4:1 contraction. There is a honeycomb also at the upstream end of the wind-engineering test section. The purpose of the honeycombs is to suppress large scale lateral and vertical components of both the steady flow and the velocity fluctuations.

Both wind-tunnel honeycombs are constructed from stacked 600-mm lengths of ϕ100 mm galvanised steel storm-water pipe. The length complies with Mehta and Bradshaw's [4] recommended L/D ratio of between 6 and 8. In the wind-engineering section, the honeycomb has 969 cells and, in the larger 5.5×4.0 m^2 duct, the honeycomb has about 2500 cells.

Screens

The wire-mesh screens installed between the honeycomb and the contraction have an open-area ratio of 62.4%, a wire pitch of M=1.67 mm and a spacing of 600 mm or 359M. The turbulence intensity in the aerodynamics test section can be estimated from an empirical relationship for the decay of grid turbulence. This relationship, found by Mohamed and LaRue [5], is

$$\left(\frac{u'}{U}\right)^2 \approx A\left(\frac{x}{M}\right)^{-1.3} \tag{10}$$

where, for the open-area ratio and Reynolds numbers of interest, $A \approx 450$. To allow for increasing flow speed through the contraction, x is calculated using

$$x = U(0)\int_0^L U(x)^{-1}dx \tag{11}$$

Equation 10 gives a test-section turbulence intensity of approximately 0.15%. The contraction area ratio of 4:1 should, in theory, give a further reduction by a factor of 2.

Diffusers

It is important that the wind-tunnel diffusers have maximum pressure recovery and a minimum of non-uniformity and unsteadiness in their outlet flows. Briefly, it is necessary to avoid boundary-layer separation in the diffusers and, as shown in the design charts of Reneau et al. [7] (Figure 10), this requires a diffuser angle 2ϕ (defined in Figure 2) of no more than 7°.

The large diffuser is divided by splitter plates into 4 channels of equal width. Without these splitter plates, the effective diffuser angle is about 30°, giving large-scale transitory separation

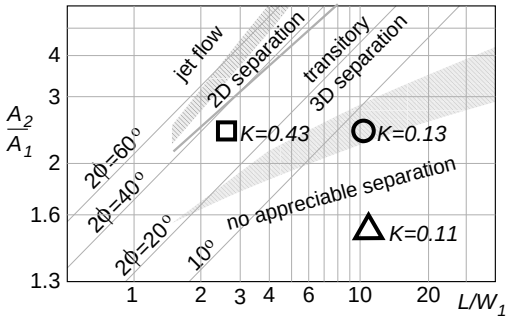

Figure 10: Simplified design chart for two-dimensional diffusers [7] showing approximate flow regime and loss coefficient (K) for the large diffuser without splitter plates (□), with splitter plates (◯), and for the fan-discharge diffusers fitted with tailcones (△).

and a loss coefficient of about 0.43. The design charts indicate that, with splitter plates, there should be almost "no appreciable separation" and a loss coefficient of about 0.13.

At present, the fan hubs are not fitted with tailcones, and so significant energy loss might be expected in the fan-discharge diffusers, perhaps with a loss coefficient (K) as high as 0.5. As illustrated in the design chart, Figure 10, the fitting of tailcones is expected to eliminate separation, thus giving a reduced in loss coefficient and a more uniform, steadier flow in the wind engineering section.

Acknowledgements

The wind tunnel was designed and constructed with the financial support of Premier's Science and Research Fund (Government of South Australia), The Sir Ross and Sir Keith Smith Fund, and the University of Adelaide.

References

[1] Bell, J. H. and Mehta, R. D., Contraction design for small low-speed wind tunnels, Technical Report 84, Joint Institute for Aernautics and Acoustics, 1988.

[2] Chmielewski, G. E., Boundary-layer considerations in the design of aerodynamic contractions, *Journal of Aircraft*, **11**, 1974, 435–438.

[3] Collar, A. R., Some experiments with cascades of aerofoils, R&M No. 1768, Aeronautical Research Council, 1936.

[4] Mehta, R. D. and Bradshaw, P., Design rules for small low speed wind tunnels, *Aeronautical Journal*, **73**, 1979, 443–449.

[5] Mohamed, M. S. and LaRue, J. C., The decay power law in grid-generated turbulence, *Journal of Fluid Mechanics*, **219**, 1990, 195–214.

[6] Patterson, G. N., Note on the design of corners in duct systems, R&M, No. 1773, Aeronautical Research Council, 1936.

[7] Reneau, L. R., Johnston, J. P. and Kline, S. J., Performance and design of straight, two-dimensional diffusers, *Journal of Basic Engineering*, **89D**, 1967, 141–150.

[8] Salter, C., Experiments on thin turning vanes, R&M, No. 2469, Aeronautical Research Council, 1952.

[9] Stratford, B. S., The prediction of separation of the turbulent boundary layer, *Journal of Fluid Mechanics*, **5**, 1959, 1–16.